Applied Physics Letters

RESEARCH ARTICLE | DECEMBER 12 2022

Enhancement of high temperature capacitive performance of sulfone-containing polyimide by suppressing carrier transport

Xue-Jie Liu; Ming-Sheng Zheng; Qian Wang; George Chen; Jun-Wei Zha

Appl. Phys. Lett. 121, 243902 (2022)
https://doi.org/10.1063/5.0132914

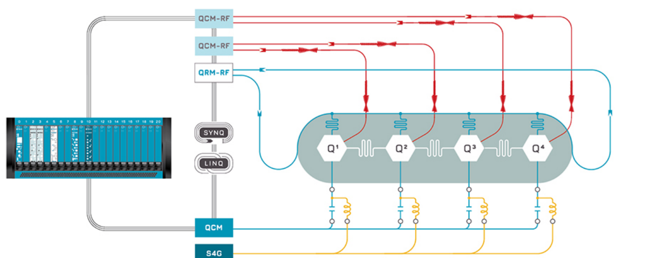

Enhancement of high temperature capacitive performance of sulfone-containing polyimide by suppressing carrier transport

Cite as: Appl. Phys. Lett. **121**, 243902 (2022); doi: 10.1063/5.0132914
Submitted: 31 October 2022 · Accepted: 30 November 2022 ·
Published Online: 12 December 2022

View Online Export Citation CrossMark

Xue-Jie Liu,[1] Ming-Sheng Zheng,[1,2,a)] Qian Wang,[3] George Chen,[4] and Jun-Wei Zha[1,2,a)]

AFFILIATIONS

[1]School of Chemistry and Biological Engineering, University of Science & Technology Beijing, Beijing 100083, People's Republic of China
[2]Shunde Graduate School of University of Science and Technology Beijing, Shunde 528399, People's Republic of China
[3]School of Electrical Engineering, Xi'an University of Technology, Xi'an 710048, People's Republic of China
[4]Department of Electronics and Computer Science, University of Southampton, Southampton SO17 1BJ, United Kingdom

[a)]Authors to whom correspondence should be addressed: zhengms@ustb.edu.cn and zhajw@ustb.edu.cn

ABSTRACT

With the increasing demand for safe operation in harsh environments, polymer dielectric capacitors with high energy density (U_e) and charge-discharge efficiency (η) operating at high temperatures are urgently needed. In this work, the sulfone group-containing polyimide (SO_2PI) film with optimal imidization degree is prepared by regulating the kinetics of imidization reaction. The functional groups obtained by partial imidization enable polyimide to achieve excellent energy storage performance, and it is found that the presence of sulfone groups is beneficial for the further improvement of η. The optimal SO_2PI film achieves a U_e of 2.40 J cm^{-3} at 400 MV m^{-1} and 150 °C, while it maintains a high η of 92%. Moreover, its preparation process without any additional modification steps matches commercial production equipment, indicating a simple and effective strategy for fabrication of a high-performance dielectric film. Thus, this work exhibits great potential in the field of high temperature energy storage.

As an energy storage device, a polymer film capacitor has numerous advantages such as high power density, excellent voltage resistance, low loss, and outstanding safety; thus, it had been widely used in electronic power systems such as power grids, electric vehicles, and aerospace. Biaxially oriented polypropylene (BOPP) is the preferred choice for capacitor films due to its high breakdown strength (E_b) >700 MV m^{-1}, low dielectric loss (tan δ) ≈ 0.02%, and ease of processability.[1–3] However, low dielectric permittivity ($\varepsilon_r \approx 2.2$) of a BOPP film makes it difficult to further improve the energy density (U_e). Moreover, the U_e and charge–discharge efficiency (η) of BOPP films decrease sharply with increasing temperature. The BOPP film can only operate at temperatures below 105 °C, even if a secondary cooling system is equipped. Therefore, it is urgent to develop high temperature polymer dielectrics with high capacitive performance.[4–7]

A high glass transition temperature (T_g) is a prerequisite for polymer dielectrics to operate at high temperatures. Thus, a series of high temperature polymers, such as polyimide (PI, $T_g > 300$ °C), polyetherimide (PEI, $T_g \approx 217$ °C) and polycarbonate (PC, $T_g \approx 150$ °C), have been developed. The existence of rigid structures, such as benzene ring, in the molecular chains results in excellent thermal stability.[8–11] However, a large number of benzene rings containing π-π conjugated structure are conducive to the formation of electron transport channels, causing high conduction loss, especially at high temperatures. For example, the η of typical PI (Kapton) films is only less than 20% at 150 °C and 300 MV m^{-1}, which is attributed to the increased conduction loss exponentially at high temperatures.[12] Therefore, high temperature polymer dielectrics should not only have high T_g, but also have low energy loss at high temperatures. Dong *et al.*[13] prepared a polymer film with a laminated structure composed of Al_2O_3 layers and PI layers, which restrained the charge injection of electrodes and reduced the conductivity of the film. An U_e of 1.59 J cm^{-3} was obtained with a η over 90% at 200 °C. Ai *et al.*[14] applied HfO_2 with large bandgap and medium ε_r into the PI matrix to prepare 5 vol. % HfO_2/PI composites, which obtained a high U_e and η of 1.21 J cm^{-3} and 91.0% at 150 °C, respectively. The design of intrinsic PIs has also received extensive attention.[15,16] Zhu *et al.*[17] introduced two ortho-position aromatic nitrile groups into the PI backbone. The polarization motion of nitrile groups was restricted, leading to the reduction of tan δ. The designed PI exhibited a high ε_r of 4.80 at 1 kHz, a low tan δ of 1.57×10^{-3}, and the maximum U_e of $1.023\,\mathrm{J\,cm^{-3}}$. The strategies discussed above improved the energy storage performance by reducing energy loss, but the following issues cannot be ignored: the agglomeration of functional fillers in the polymer causes physical defects; the preparation of multi-layer structure composites is usually complicated or high cost; the synthesis of monomers is time-consuming and accompanied by the generation of by-products, which requires extensive explorations before practical application. All of the above conditions reduce the possibility of large-scale application of films.[18–20]

In our previous work, a series of PI films with different contents of –COOH/–CONH– groups were prepared by tuning the kinetics of imidization reaction.[21] It has been proved that an appropriate ratio of –COOH/-CONH– groups in PI is helpful for the enhancement of U_e and η. This film preparation method matches the commercial manufacturing process and, therefore, has the possibility of practical application. In addition, the introduction of sulfone (–SO_2–) groups has been proved to improve the η by suppressing the loss at high temperatures.[22–24] The highly polar sulfone groups with a dipole moment of 4.3 Debye into the polymer backbone can further improve the ε_r.[25] In this work, sulfone group-containing polyimide (SO_2PI) is obtained, and its thermal imidization process is optimized simultaneously. The SO_2PI film with proper imidization degree (ID, 90%) obtains the maximum U_e of $5.14\,\mathrm{J\,cm^{-3}}$ with a η of 90% at 25 °C and $535\,\mathrm{MV\,m^{-1}}$. Remarkably, a high U_e of $2.4\,\mathrm{J\,cm^{-3}}$ is obtained with an η of 92% at 150 °C and $400\,\mathrm{MV\,m^{-1}}$. This facile method provides the possibility for the application of PI films in the field of film capacitors.

The conventional two-step thermal imidization method is used to fabricate SO_2PI films with different IDs by adjusting the thermal imidization temperature as shown in Figs. 1(a) and 1(b) (see the

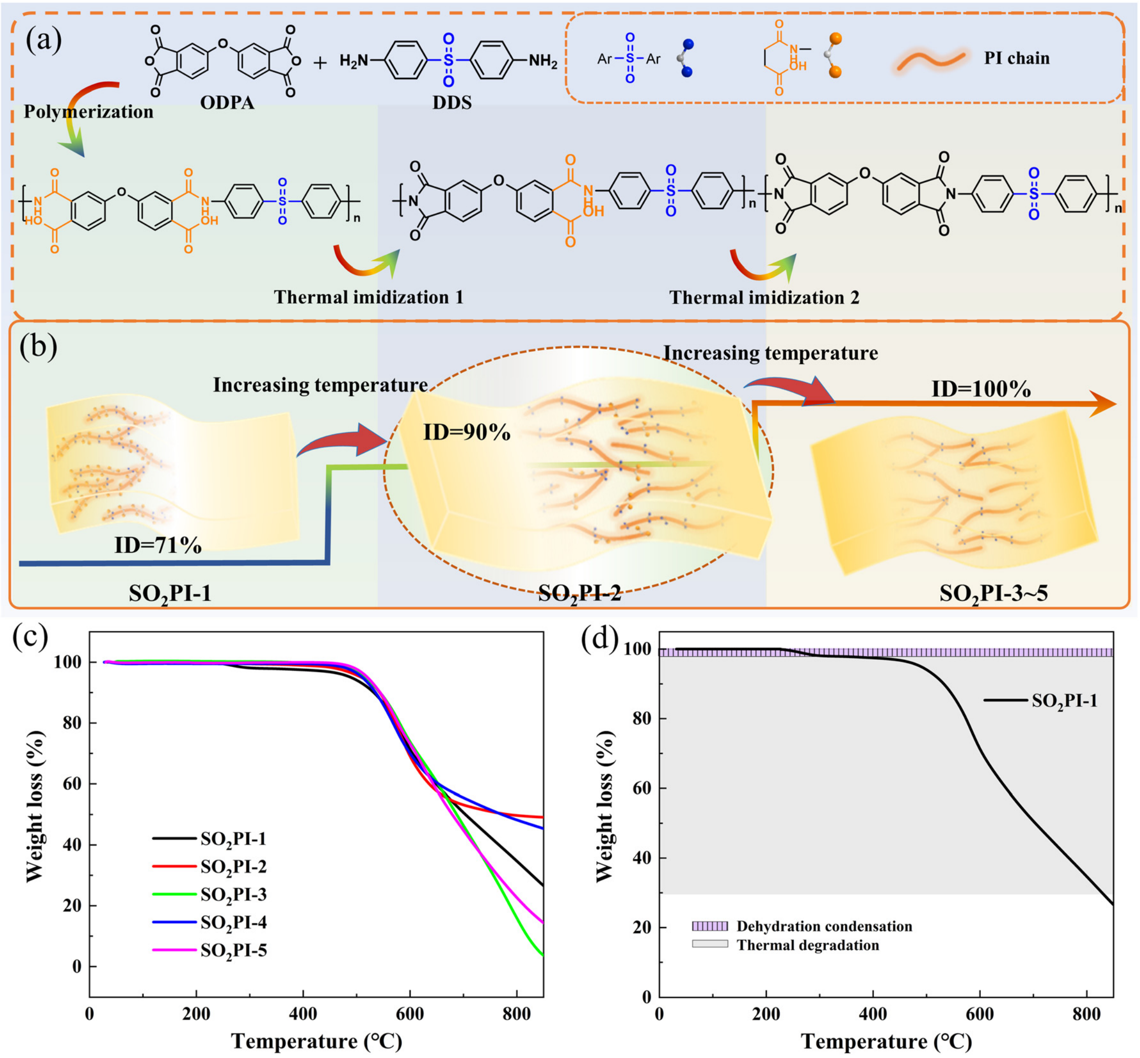

FIG. 1. (a) Synthesis process and (b) schematic of SO_2PI films with different IDs. (c) TGA curves of the SO_2PI films with different IDs. (d) Two steps of the thermal weight loss process for the SO_2PI-1 film obtained by TGA.

supplementary material for the experimental section). Fourier transform infrared spectroscopy (FTIR) of SO_2PI films with different IDs is shown in Fig. S1, and all of the SO_2PI films contain characteristic absorption peaks of PI, including asymmetric and symmetric stretching C=O at 1780 and 1730 cm^{-1}, C–N stretching at 1370 cm^{-1} and C = O bending of imide ring at 748 cm^{-1}, respectively.

The characteristic absorption peak at 1533 cm^{-1} for N-H deformation coupled with C–N stretching of the amide linkage in polyamic acid (PAA) can be observed only in the SO_2PI-1 film. The characteristic absorption peaks of PAA in FTIR spectra are difficult to identify when the ID is close to 80%.[26] In addition, the IDs of SO_2PI-1∼5 films can be accurately calculated from the thermal gravimetric analyzer (TGA) results as shown in Fig. 1(c).[27,28] When the N-N-Dimethylacetamide (DMAc) solvent and water are completely evaporated, the total weight loss for the partially imidized SO_2PI films consists of two steps: dehydration condensation of PAA (the first step) and thermal decomposition of PI (the second step). The weight loss for SO_2PI films with complete imidization only involves the second step. As illustrated in Fig. 1(d), taking the SO_2PI-1 film as an example, the ID can be obtained by the following equation using the weight lost in the first step:

$$\text{Weight loss\%} = \frac{\mathrm{M(2H_2O)} \times (100\% - \mathrm{ID})}{\mathrm{M(PAA)} - \mathrm{M(2H_2O)} \times \mathrm{ID}} \times 100\%, \qquad (1)$$

where M(PAA) and M(H_2O) are the molecular weight of the PAA repeating unit and H_2O, respectively. The IDs of SO_2PI-1 ∼ 5 films are shown in Table S1. According to the reaction kinetics mechanism of thermal imidization, the degree of the imidization reaction depends on temperature, which stems from the reduced mobility of molecular chains. Figure S2 reveals the relationship between ID and processing temperature. The ID of SO_2PI films increases from 71% to 100% with the raised processing temperature. The SO_2PI films achieve "complete imidization" at about 300 °C, which has been proved by previous works.[29–31] TGA curves depict that the thermal decomposition temperature at 5% weight loss ($T_{d5\%}$) of SO_2PI films is displayed around 500 °C, indicating the excellent thermal stability. SO_2PI-1 ∼ 2 films continue to undergo imidization reaction during the TGA test. Dehydration condensation of -NH- and -OH bonds in SO_2PI-1 ∼ 2 films leads to weight loss at lower temperatures. The $T_{d5\%}$ and $T_{d10\%}$ gradually increase from the SO_2PI-1 film to the SO_2PI-5 film due to the increase in ID and the close packing of molecular chains. Figure S3 exhibits that the T_g of SO_2PI-1 ∼ 5 films with ID (≥71%) is stable at about 299 °C. It is considered that SO_2PI films have a higher T_g than conventional PI films due to the addition of rigid -SO_2– groups.[21]

Figure 2(a) describes the ε_r and tanδ of SO_2PI-1 ∼ 5 films as a function of frequency at 25 °C. Due to the introduction of sulfone groups, the "completely imidized" SO_2PI-3 ∼ 5 films obtain a higher ε_r

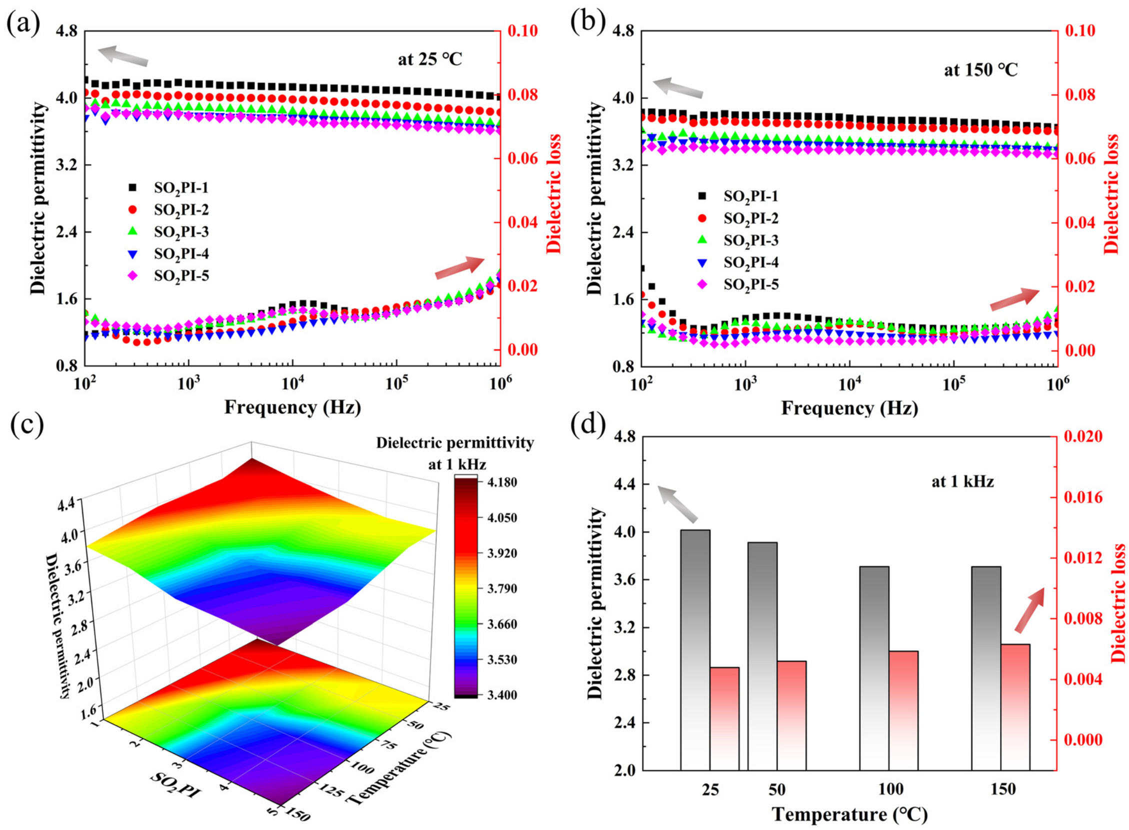

FIG. 2. Dielectric properties of the SO_2PI films with different IDs: (a) at 25 and (b) 150 °C. (c) The dielectric permittivity of the SO_2PI films as a function of temperature. (d) Dielectric properties of the SO_2PI-2 film at different temperatures and 1 kHz.

of 3.8 at 1 kHz compared with Kapton films ($\varepsilon_r \sim 3.2$).[32,33] Then, ε_r of SO_2PI films further increases with decreased ID due to the enhanced dipolar polarization derived from the increase in –COOH/–CONH– polar groups. The SO_2PI-1 film with the lowest ID of 71% leads to the highest ε_r of 4.17 at 1 kHz. Figures S4 and 2(b) illustrate that the ε_r of the SO_2PI-1 film at 1 kHz are 4.02, 3.97, and 3.79 at 50, 100, and 150 °C, respectively. Figure 2(c) demonstrates that ε_r of all SO_2PI films decreases with increasing temperature. Taking the SO_2PI-2 film as an example, the ε_r decreases slightly before 100 °C and then remains stable, while tanδ increases slightly with temperature at 1 kHz [see Fig. 2(d)]. Moreover, ε_r of all SO_2PI films decrease with increasing frequency, mainly because the rotation of the dipole cannot catch up with the change in an alternating electric field at high frequencies. At 25 °C, tanδ of SO_2PI films increases at high frequencies due to polarization relaxation. The gradual decrease in tanδ at high frequencies with increasing temperature is attributed to the more active dipoles at higher temperature.

The two-parameter Weibull statistical distribution is used to analyze the breakdown strength of SO_2PI films, as shown as

$$P = 1 - \exp\left[-\left(\frac{E}{E_b}\right)^{\beta}\right], \tag{2}$$

where P is the probability of electrical failure, E is the experimentally obtained breakdown strength, E_b represents the characteristic breakdown strength with a breakdown probability of 63.2%, and β is the shape parameter. Figures 3(a) and 3(b) exhibit the Weibull distribution of breakdown strength of SO_2PI films at 25 and 150 °C. Compared with the "completely imidized" SO_2PI-3 film, the SO_2PI-2 film with proper ID of 90% obtains a higher E_b of 535 and 483 MV m^{-1} at 25 and 150 °C, respectively. As shown in Fig. 3(c), all of SO_2PI films exhibit the decreased E_b as a function of the testing temperature. Since more charges are activated and move directionally at high temperatures and high electric fields, the leakage current is multiplied, which greatly reduces E_b. Figure S5(c) shows that the E_b of SO_2PI films first increases and then decreases as a function of ID at different temperatures. An appropriate amount of polar groups in the SO_2PI-2 film brings about an improvement in E_b, which is consistent with our previous work.[21] On the one hand, the proper –SO_2– and –COOH–/–CO–NH– groups act as traps to suppress the carrier mobility and, thus, enhance E_b.[34–36] On the other hand, the introduction of excessive polar groups in the SO_2PI-1 film leads to trap overlap, which is conducive to the carrier migration process. Owing to the damage of polymer chains caused by the excessive temperature, the SO_2PI-5 film with an imidization temperature of 400 °C obtains the lowest E_b of 407 and 368 MV m^{-1} at 25 and 150 °C, respectively.

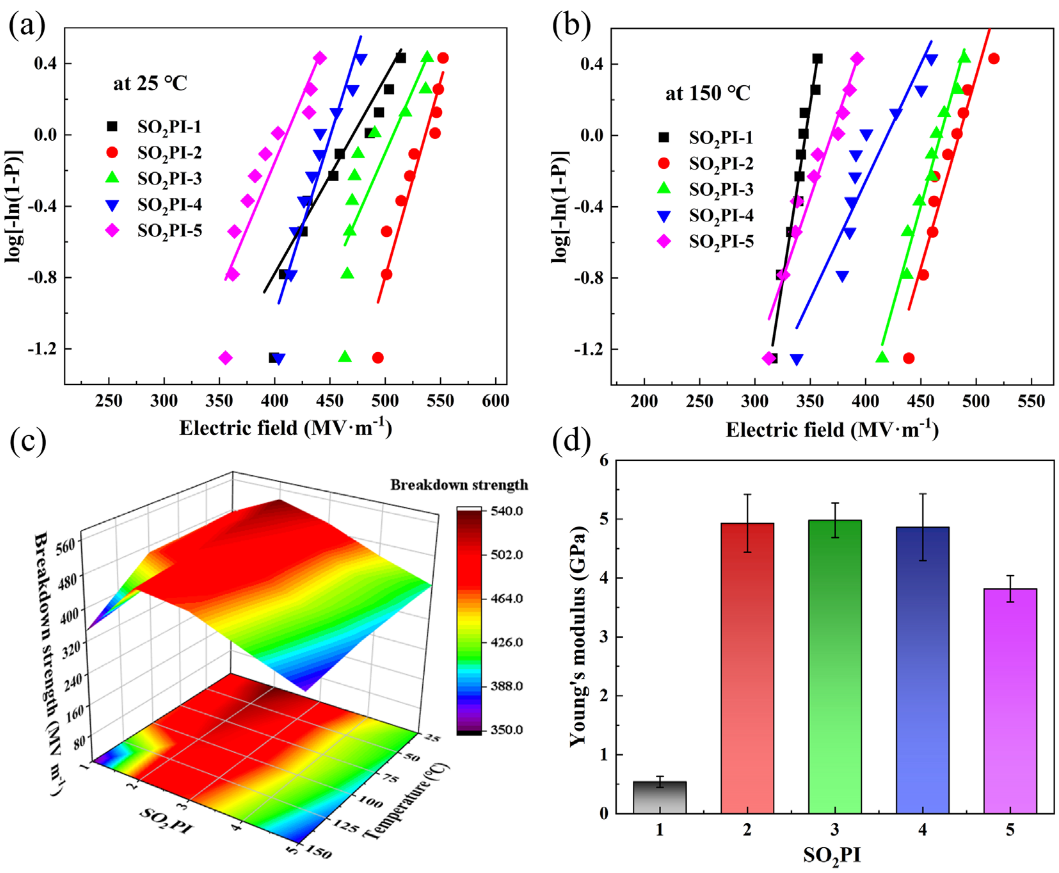

FIG. 3. Weibull distribution of breakdown strength of the SO_2PI films with different IDs at (a) 25 and (b) 150 °C. (c) E_b of the SO_2PI films with different IDs as a function of the testing temperature. (d) Young's modulus of the SO_2PI films with different IDs.

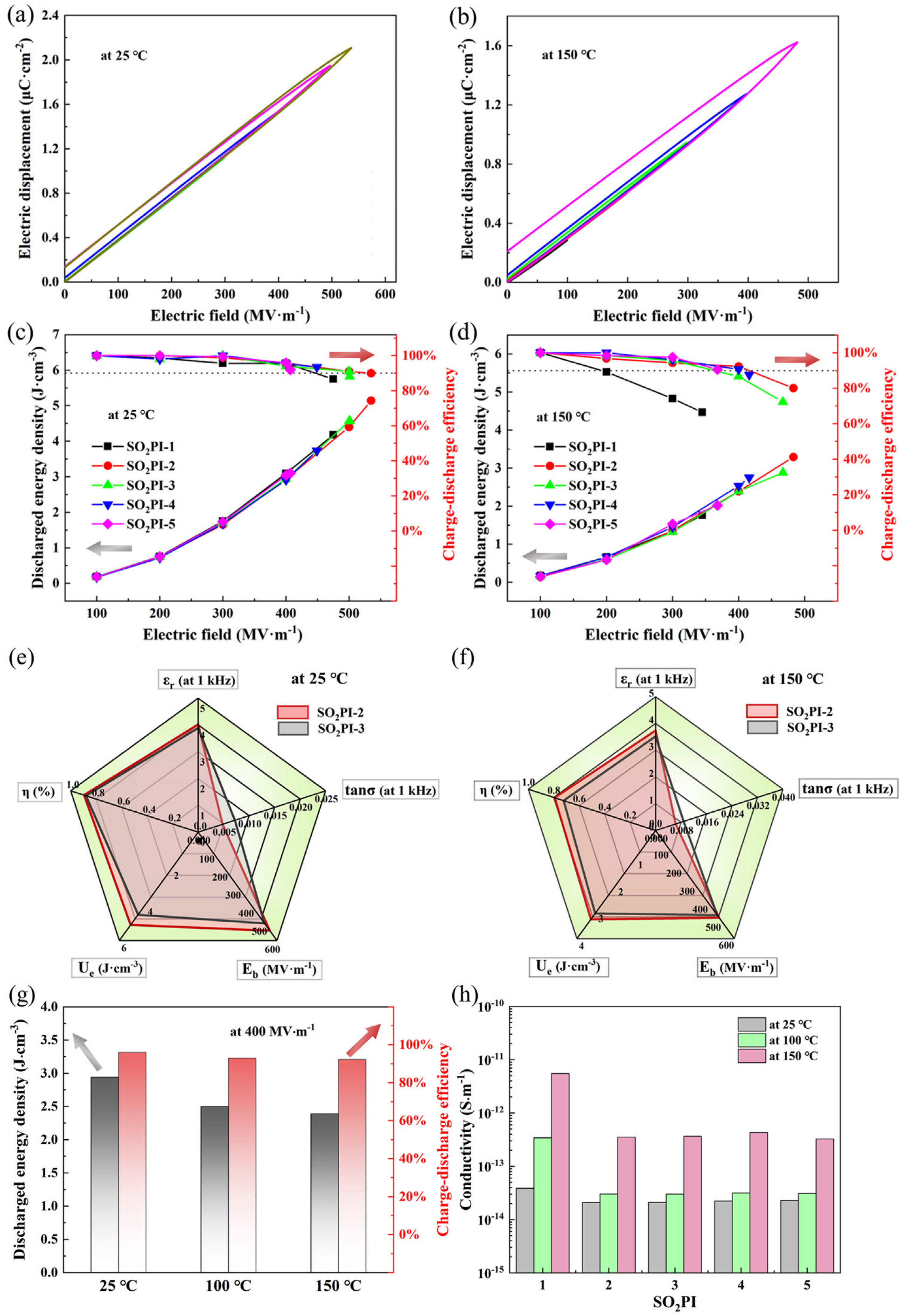

FIG. 4. D–E loops of the SO_2PI-2 film with different IDs: (a) at 25 °C and (b) at 150 °C. U_e and η of the SO_2PI films with different IDs at (c) at 25 and (d) 150 °C. The radar plots of the SO_2PI-2 film and SO_2PI-3 film at (e) 25 and (f) 150 °C. (g) U_e and η of the SO_2PI-2 film at 400 MV m^{-1} and (h) conductivity of the SO_2PI films at different temperatures.

Under the action of the electric field, the attraction between positive and negative charges on both sides of the dielectric forms electrostatic compression force, and the resulting electromechanical breakdown is a factor of dielectric failure. The electromechanical breakdown strength (E_{EM}) and Young's modulus (Y) have the following relationship:

$$E_{EM} = 0.606\sqrt{\frac{Y}{\varepsilon_0 \varepsilon_r}}, \tag{3}$$

where ε_0 is the vacuum permittivity, which is 8.85×10^{-12} F m^{-1}. Figure 3(d) shows that Young's modulus of SO_2PI films first increases and then decreases with the increased ID. The SO_2PI-2 film has the highest Young's modulus of about 5 GPa to resist the effects of E_{EM}.[37] Young's modulus of the SO_2PI-1 film is significantly lower than other SO_2PI films. The introduction of excess polar –COOH/–CO–NH– groups weakens the binding force of molecular chains, resulting in poor mechanical property.

Figures 4(a), 4(b), and S6 show the *D-E* loops of the SO_2PI-2 film under different electric fields. In the temperature range of 25-150 °C, the SO_2PI-2 film exhibits thin D–E loops under 400 MV m^{-1}, indicating low residual displacement. The maximum electric displacement of the SO_2PI-2 film is 2.11 and 1.62 μC cm^{-2} at 25 and 150 °C, respectively. The U_e and η of SO_2PI-1∼5 films are obtained from the *D–E* loops as shown in Figs. 4(c), 4(d), and S6. For a linear dielectric, U_e can be expressed by the following equation:

$$U_e = \frac{1}{2}\varepsilon_0\varepsilon_r E_b^2. \quad (4)$$

It can be seen that U_e is proportional to the square of E_b, thereby the improvement of E_b is more critical to the increasing U_e. The SO_2PI-2 film with the highest E_b achieves the maximum U_e of 5.14 J cm^{-3} with the η of 90% at 25 °C. Notably, the SO_2PI-2 film gains a higher U_e of 3.29 J cm^{-3} with the η of 80% compared with the "completely imidized" SO_2PI-3 film [the U_e of 3.07 J cm^{-3} and η of 72%] at 150 °C. At this time, the SO_2PI-1 film with lower ID has a reduced U_e of 1.76 J cm^{-3} with the η of 66%, and the decreased U_e and η of SO_2PI-4 and SO_2PI-5 films are also observed. Figures 4(e) and 4(f) demonstrate the comprehensive capacitive performance of SO_2PI films. The SO_2PI-2 film has more excellent E_b, U_e, and η compared with SO_2PI-3 films. It is worth noting that the processing temperature of SO_2PI-2 films decreases by 50 °C, while the capacitance performance increases, which is beneficial to reduce the energy consumption in the preparation process.

Compared with the previous work, the improved η of SO_2PI films mainly originates from the introduction of –SO_2– groups, especially at high temperatures.[21] The higher polar –SO_2– groups have stronger electrostatic forces compared with the –COOH–/–CO-NH– groups, making it easier to capture charge carriers, resulting in lower conductivity and higher η.[22,23,35,38–40] At 400 MV m^{-1}, the η of the SO_2PI-2 film is only reduced from 96% at 25 °C to 92% at 150 °C, indicating good temperature stability [see Fig. 4(g)]. Moreover, the "completely imidized" SO_2PI-3 film obtains a lower η of 86% at 400 MV m^{-1} and 150 °C, which shows that an appropriate amount of –COOH–/–CO–NH– groups also help it to improve the η.

The suppressed conductivity ensures lower energy loss to improve efficiency, which is critical for reducing thermal breakdown of capacitor films.[41] As shown in Fig. 4(h), the conductivity of SO_2PI films decreases first and then increases with an increase in ID, consistent with the variation of E_b. The SO_2PI-2 film maintains a lower conductivity at different temperatures, increasing from $2.09\cdot10^{-14}$ S m^{-1} at 25 °C to $3.52\cdot10^{-13}$ S m^{-1} at 150 °C. The conductivity of the SO_2PI-1–SO_2PI-5 film increases by 141, 15, 16, 18, and 14 times from 25 to 150 °C, respectively. The conductivity of the SO_2PI-1 film increases substantially with raising temperature due to the fact that more charges are activated at high temperatures, which rapidly reduces the E_b and η.

A fast charge-discharge experiment is implemented to evaluate the power density of the SO_2PI-2 film.[42,43] The discharge time is defined as the time when the U_e reaches 90% of the discharge profiles as shown in Fig. 5(a). The discharge time of SO_2PI-2 film and BOPP film is 11.2 μs and 10.6 μs, respectively.The power density is obtained by calculating the ratio of 90% of the final energy density to the discharge time. Figure 5(b) reveals that the SO_2PI-2 film exhibits a higher power density of 67.1 kW cm^{-3}, which is 140% of the BOPP film (47.2 kW cm^{-3}).

In summary, the high-temperature capacitive performance of the SO_2PI film is improved by optimizing the thermal imidization process of polyamic acid. First, both the –COOH/–CN–OH– and –SO_2– groups promote the dielectric permittivity by enhancing the dipole polarization. These polar groups also act as traps to hinder the carrier migration process, thereby improving the breakdown strength. Then, the introduction of sulfone groups further reduces the energy loss at high temperatures. Thus, the SO_2PI film obtains a high U_e and η of 5.14 J cm^{-3} and 90% at 25 °C, respectively. It is worth noting that a high U_e of 2.40 J cm^{-3} with a η of 92% is still achieved at 400 MV m^{-1} and 150 °C. Finally, the high power density of SO_2PI-2 films is also confirmed. The simple fabrication process and corresponding high performance show the potential application in the field of high-temperature capacitors.

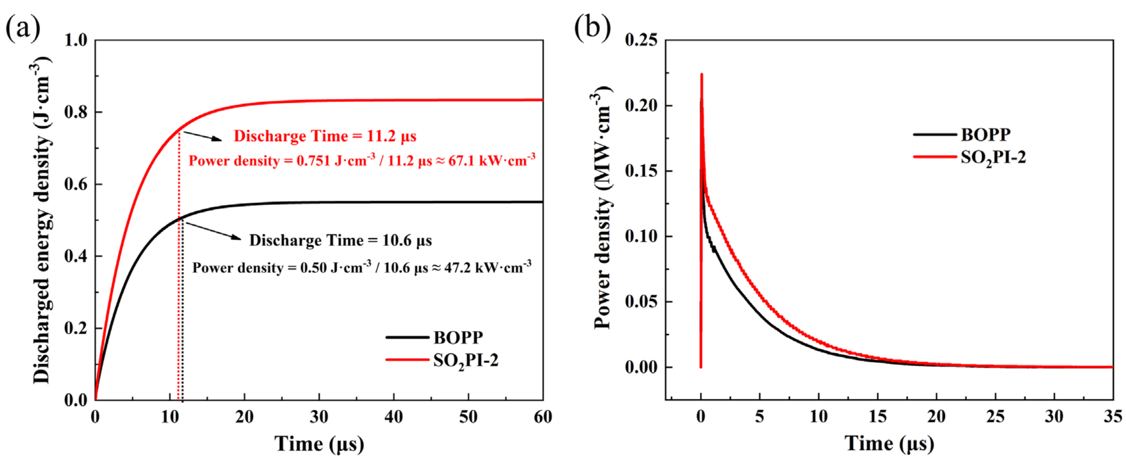

FIG. 5. (a) Discharge time and (b) power density as a function of time of the BOPP and SO_2PI-2 film.

See the supplementary material for the information on the experimental part, characterization results by FTIR and DSC, thermal properties of SO_2PI films, dielectric properties, and energy storage performance of SO_2PI films at 50 and 100 °C.

This work was financially supported by the National Natural Science Foundation of China (Nos. 51977114 and 52277022), the Scientific and Technological Innovation Foundation of Foshan (Nos. BK21BE006 and BK22BE009), and the State Key Laboratory of Power System and Generation Equipment (No. SKLD21 KM08).

AUTHOR DECLARATIONS

Conflict of Interest

The authors have no conflicts to disclose.

Author Contributions

Xue-Jie Liu: Conceptualization (equal); Data curation (equal); Formal analysis (equal); Visualization (equal); Writing – original draft (equal). **Ming-Sheng Zheng:** Conceptualization (equal); Formal analysis (equal); Methodology (equal); Supervision (equal); Writing – review & editing (equal). **Qian Wang:** Resources (equal); Software (equal); Validation (equal). **George Chen:** Project administration (equal); Resources (equal); Software (equal). **Jun-Wei Zha:** Conceptualization (equal); Funding acquisition (equal); Methodology (equal); Project administration (equal); Supervision (equal); Writing – review & editing (equal).

DATA AVAILABILITY

The data that support the findings of this study are available from the corresponding authors upon reasonable request.

REFERENCES

[1]H. Li, Y. Zhou, Y. Liu, L. Li, Y. Liu, and Q. Wang, Chem. Soc. Rev. **50**, 6369 (2021).
[2]B. Fan, M. Zhou, C. Zhang, D. He, and J. Bai, Prog. Polym. Sci. **97**, 101143 (2019).
[3]M. S. Zheng, Y. T. Zheng, J. W. Zha, Y. Yang, P. Han, Y. Q. Wen, and Z. M. Dang, Nano Energy **48**, 144 (2018).
[4]Q. Li, F. Z. Yao, Y. Liu, G. Zhang, H. Wang, and Q. Wang, Annu. Rev. Mater. Res. **48**, 219 (2018).
[5]D. Tan, L. Zhang, Q. Chen, and P. Irwin, J. Electron. Mater. **43**, 4569 (2014).
[6]B. Fan, F. Liu, G. Yang, H. Li, G. Zhang, S. Jiang, and Q. Wang, IET Nanodielectr. **1**, 32 (2018).
[7]Q. K. Feng, S. L. Zhong, J. Y. Pei, Y. Zhao, D. L. Zhang, D. F. Liu, Y. X. Zhang, and Z. M. Dang, Chem. Rev. **122**, 3820 (2022).
[8]X. J. Liu, M. S. Zheng, G. Chen, Z. M. Dang, and J. W. Zha, Energy Environ. Sci. **15**, 56 (2022).
[9]B. Q. Wan, M. S. Zheng, X. X. Yang, D. Dong, Y. Li, Y. W. Mai, and J. W. Zha, Energy Environ. Mater. **0**, e12427 (2022).
[10]X. D. Dong, M. S. Zheng, B. Q. Wan, X. J. Liu, H. P. Xu, and J. W. Zha, Materials **14**, 6266 (2021).
[11]L. Sun, Z. C. Shi, B. L. He, H. L. Wang, S. A. Liu, M. H. Huang, J. Shi, D. Dastan, and H. Wang, Adv. Funct. Mater. **31**, 2100280 (2021).
[12]Q. Li, L. Chen, M. R. Gadinski, S. Zhang, G. Zhang, H. U. Li, E. Iagodkine, A. Haque, L. Chen, T. N. Jackson, and Q. Wang, Nature **523**, 576 (2015).
[13]J. F. Dong, R. C. Hu, X. W. Xu, J. Chen, Y. J. Niu, F. Wang, J. Y. Hao, K. Wu, Q. Wang, and H. Wang, Adv. Funct. Mater. **31**, 2102644 (2021).
[14]D. Ai, H. Li, Y. Zhou, L. Ren, Z. Han, B. Yao, W. Zhou, L. Zhao, J. Xu, and Q. Wang, Adv. Energy Mater. **10**, 1903881 (2020).
[15]H. Tong, J. Fu, A. Ahmad, T. Fan, Y. Hou, and J. Xu, Macromol. Mater. Eng. **304**, 1800709 (2019).
[16]R. Ma, A. F. Baldwin, Ch. Wang, I. Offenbach, M. Cakmak, R. Ramprasad, and G. A. Sotzing, ACS Appl. Mater. Interfaces **6**, 10445 (2014).
[17]T. Zhu, Q. Yu, W. Zheng, R. Bei, W. Wang, M. Wu, S. Liu, Z. Chi, Y. Zhang, and J. Xu, Polym. Chem. **12**, 2481 (2021).
[18]J. W. Zha, M. S. Zheng, B. H. Fan, and Z. M. Dang, Nano Energy **89**, 106438 (2021).
[19]H. Luo, X. Zhou, C. Ellingford, Y. Zhang, S. Chen, K. Zhou, D. Zhang, C. R. Bowen, and C. Wan, Chem. Soc. Rev. **48**, 4424 (2019).
[20]X. Huang and P. Jiang, Adv. Mater. **27**, 546 (2015).
[21]X. J. Liu, M. S. Zheng, G. Wang, Y. Y. Zhang, Z. M. Dang, G. Chen, and J. W. Zha, J. Mater. Chem. A **10**, 10950 (2022).
[22]Z. Zhang, D. H. Wang, M. H. Litt, L. S. Tan, and L. Zhu, Angew. Chem., Int. Ed. **57**, 1528 (2018).
[23]Z. Zhang, J. Zheng, K. Premasiri, M. Kwok, Q. Li, R. Li, S. Zhang, M. H. Litt, X. P. A. Gao, and L. Zhu, Mater. Horiz. **7**, 592 (2020).
[24]Y. Wang, X. Huang, T. Li, Z. Wang, L. Li, X. Guo, and P. Jiang, J. Mater. Chem. A **5**, 20737 (2017).
[25]W. W. Zheng, T. Z. Yang, L. J. Qu, X. C. Liang, C. N. Liu, C. Qian, T. W. Zhu, Z. X. Zhou, C. A. Liu, S. W. Liu, Z. G. Chi, J. R. Xu, and Y. Zhang, Chem. Eng. J. **436**, 135060 (2022).
[26]W. Chen, W. Chen, B. Zhang, S. Yang, and C. Y. Liu, Polymer **109**, 205 (2017).
[27]W. K. Yang, F. F. Liu, G. M. Li, E. S. Zhang, Y. H. Xue, Z. X. Dong, X. P. Qiu, and X. L. Ji, Chin. J. Polym. Sci. **34**, 209 (2016).
[28]E. Unsal and M. Cakmak, Macromolecules **46**, 8616 (2013).
[29]M. Kotera, T. Nishino, and K. Nakamae, Polymer **41**, 3615 (2000).
[30]Y. K. Xu, M. S. Zhan, and K. Wang, J. Polym. Sci., Part B **42**, 2490 (2004).
[31]Q. K. Feng, D. F. Liu, Y. X. Zhang, J. Y. Pei, S. L. Zhong, H. Y. Hu, X. J. Wang, and Z. M. Dang, Nano Energy **99**, 107410 (2022).
[32]Y. P. Li, J. H. Yin, Y. Feng, J. L. Li, H. Zhao, C. C. Zhu, D. Yue, Y. P. Liu, B. Su, and X. X. Liu, Chem. Eng. J. **429**, 132228 (2022).
[33]Q. K. Feng, Q. Dong, D. L. Zhang, J. Y. Pei, and Z. M. Dang, Compos. Sci. Technol. **218**, 109193 (2022).
[34]H. L. Liu, B. X. Du, and M. Xiao, IEEE Trans. Dielectr. Electr. Insul. **28**, 1539 (2021).
[35]J. W. Zha, Y. H. Wu, S. J. Wang, D. H. Wu, H. D. Yan, and Z. M. Dang, IEEE Trans. Dielectr. Electr. Insul. **23**, 2337 (2016).
[36]H. Yuan, Y. Zhou, Y. J. Zhu, S. X. Hu, C. Yuan, W. B. Song, Q. Shao, Q. Zhang, J. Hu, Q. Li, and J. L. He, J. Phys. D **53**, 475301 (2020).
[37]Q. K. Feng, J. B. Ping, J. Zhu, J. Y. Pei, L. Huang, D. L. Zhang, Y. Zhao, S. L. Zhong, and Z. M. Dang, Macromol. Rapid Commun. **42**, 2100116 (2021).
[38]D. Wu, X. Zhao, X. T. Li, J. Dong, and Q. H. Zhang, Polymer **256**, 125221 (2022).
[39]C. Yuan, Y. Zhou, Y. Zhu, J. Liang, S. Wang, S. Peng, Y. Li, S. Cheng, M. Yang, J. Hu, B. Zhang, R. Zeng, J. He, and Q. Li, Nat. Commun. **11**, 3919 (2020).
[40]X. Z. He, I. Rytoluoto, R. Anyszka, A. Mahtabani, E. Saarimaki, K. Lahti, M. Paajanen, W. Dierkes, and A. Blume, IEEE Access **8**, 87719 (2020).
[41]T. D. Zhang, L. Y. Yang, C. H. Zhang, Y. Feng, J. Wang, Z. H. Shen, Q. G. Chen, Q. Q. Lei, and Q. G. Chi, Mater. Horiz. **9**, 1273 (2022).
[42]Y. Zhu, Y. Zhu, X. Huang, J. Chen, Q. Li, J. He, and P. Jiang, Adv. Energy Mater. **9**, 1901826 (2019).
[43]J. Y. Pei, S. L. Zhong, Y. Zhao, L. J. Yin, Q. K. Feng, L. Huang, D. F. Liu, Y. X. Zhang, and Z. M. Dang, Energy Environ. Sci. **14**, 5513 (2021).